ELSEVIER

Three-dimensional pharmacophore hypotheses of octopamine receptor responsible for the inhibition of sex-pheromone production in *Helicoverpa armigera*

Akinori Hirashima,* Ada Rafaeli,† Carina Gileadi,† and Eiichi Kuwano*

**Division of Bioresource and Bioenvironmental Sciences, Graduate School, Kyushu University, Fukuoka 812-8581, Japan †Department of Stored Products, Pheromone Research Laboratory, Volcani Centre, Bet Dagan 50250, Israel*

Three-dimensional pharmacophore hypotheses were built on the basis of a set of nine octopamine (OA) agonists responsible for the inhibition of sex-pheromone production in Helicoverpa armigera*. Of the 10 models generated by the program Catalyst/Hypo, hypotheses including hydrogen-bond acceptor (HBA), hydrophobic (Hp), and hydrophobic aliphatic (HpAl) features were considered important and predictive in evaluating OA agonists. An HBA and four hydrophobic features are the minimum components of an effective OA agonist-binding hypothesis, which resembles the results of binding activity to locust OAR3. Active agonists mapped well onto all of the features of the hypothesis, such as HBA, Hp, and HpAl features. On the other hand, inactive compounds lacking binding affinity were shown to be poorly capable of achieving an energetically favorable conformation shared by the active molecules in order to fit the 3D chemical feature pharmacophore models. Those hypotheses are considered useful in designing new leads for more active compounds. Further research on the comparison of models from agonists may help elucidate the mechanisms of OA receptor–ligand interactions. © 1999 by Elsevier Science Inc.*

Color Plates for this article are on pages 53–54.

Address reprint requests to: Akinori Hirashima, Division of Bioresource and Bioenvironmental Sciences, Graduate School, Kyushu University, Fukuoka 812-8581, Japan. Tel.: +81-92-642-2856; Fax: +81-92-642-2864. E-mail: ahirasim@agr.kyushu-u.ac.jp

Keywords: Helicoverpa armigera, *octopamine agonist, receptor hypothesis, catalyst, pharmacophore*

INTRODUCTION

Production of the pheromone blend is under the regulation of a neuropeptide termed *pheromone biosynthesis-activating neuropeptide* (PBAN).[1–4] The direct action of PBAN has been demonstrated by studies in vitro[5–10] showing stimulation of pheromone production in the presence of synthetic peptide by isolated pheromone gland tissue. The exact tissue involved was delineated as the intersegmental membrane, which is situated between the eighth and ninth abdominal segments.[11,12] In *Helicoverpa armigera*, we have shown that octopamine (OA) and clonidine significantly inhibit the pheromonotropic action due to PBAN in intact moths and decapitated moths, as well as pheromone gland incubations in vitro.[11–13] The inhibition was also reflected in a significant inhibitory effect on intracellular cAMP levels which were stimulated in the presence of PBAN. This inhibitory action is a result of a receptor (separate from the PBAN receptor) that can be inhibited by pertussis toxin.[12] This provided evidence that this specific pheromonostatic aminergic receptor is linked to a G-inhibitory protein.

The biogenic monoamine OA, which has been found in high concentrations in various insect tissues, is the monohydroxylated analog of the vertebrate hormone noradrenaline. OA receptors are perhaps the only nonpeptide receptors whose occurrence is restricted to invertebrates. It has been found that OA is present at high concentrations in various invertebrate tissues.[14] This multifunctional and naturally occurring biogenic amine has been well

Journal of Molecular Graphics and Modelling 17, 43–50, 1999

655 Avenue of the Americas, New York, NY 10010

1093-3263/99/$–see front matter
PII S1093-3263(99)00019-4

studied and established as (1) a neurotransmitter, controlling the firefly light organ and endocrine gland activity in other insects; (2) a neurohormone, inducing mobilization of lipids and carbohydrates; (3) a neuromodulator, acting peripherally on different muscles, fat body, and sensory organs such as the corpora cardiaca and the corpora allata; and (4) a centrally acting neuromodulator, influencing motor patterns, habituation, and even memory in various invertebrate species.[15,16] The action of OA is mediated through various receptor classes, members of which are coupled to G proteins and are specifically linked to an adenylate cyclase. Thus, the physiological actions of OA have been shown to be associated with elevated levels of cyclic AMP.[17] Three different receptor classes, OAR1, OAR2A, and OAR2B, have been distinguished from nonneuronal tissues.[18] In the nervous system of the locust, a particular receptor class was characterized and established as a new class, OAR3, by pharmacological investigations of the [^{3}H]OA binding site, using various agonists and antagonists.[19–23] Much attention has been directed at the octopaminergic system as a valid target in the development of safer and selective pesticides.[24–26] Structure–activity studies of various types of OA agonists and antagonists were reported, using the nervous tissue of the migratory locust, *Locusta migratoria* L.[19–23] However, information on the structural requirements of these OA agonists and antagonists for high OA receptor ligands is still limited. The pheromonostatic receptor, acting in a neuromodulatory role, represents a novel type of octopaminergic receptor that induces an inhibitory and not a stimulatory action on adenylate cyclase. It is therefore of critical importance to provide information on the pharmacological properties of this OA receptor type and its subtypes.

Our interest in octopaminergic agonists was aroused by the results of a QSAR study using various physicochemical parameters as descriptors[27,28] or receptor surface models.[29] Furthermore, molecular modeling and conformational analysis were performed in Catalyst/Hypo[30] to gain a better knowledge of the interactions between octopaminergic antagonists[31] and OAR3 in order to identify the conformations required for binding activity. A similar procedure was repeated using OA agonists.[32] The current work is aimed at generating 3D chemical function-based hypotheses from the set of OA agonists responsible for the inhibition of sex-pheromone production in *H. armigera.*

SYNTHESIS OF OCTOPAMINE AGONISTS

The compounds reported here have been prepared by the first author according to the Hirashima et al.[25]: EPIT 9 was synthesized by the cyclization of monoethanolamine hydrogen sulfate with 2,6-diethylphenylisothiocyanate in the presence of sodium hydroxide. AIOs (**1**, **2**, **10**, and **11**) (see Figure 1), BAOs (**3** and **4**), and BAOF (**27**) were obtained by cyclodesulfurizing the corresponding thiourea with yellow mercuric oxide. CBAT (**7**), DPIT (**8**), AITs (**19**–**23**), AITM (**24**), and AITT (**25**) were synthesized by cyclization of the corresponding thiourea with concentrated hydrogen chloride. NC (**6**) was prepared by refluxing the corresponding aniline and 1-acetyl-2-imidazolidone in phosphoryl chloride followed by hydrolysis. The structures of the compounds were confirmed by ^{1}H and ^{13}C NMR measured with a JEOL JNM-EX400 spectrometer at 400 MHz, tetramethyl silane (TMS) being used as an internal standard for ^{1}H NMR and by elemental analytical data. Clonidine (**5**) was obtained from Sigma (St. Louis, MO).

BIOLOGICAL ASSAY

The compounds have been assayed at the Volcani Centre in Israel. The first author engaged in preliminary experiments[33] at the Volcani Centre, where A. Rafaeli was his host during his sabbatical leave. More detailed biochemical work was done by his coauthors at the Volcani Centre, and he did all QSAR calculations himself at Kyushu University in Japan.

Insect culture

The study was conducted on *H. armigera.* The larvae were raised on an artificial diet at a constant temperature of 25°C and a 14:10 (light:dark) photoperiod as reported previously. Pupae were sexed and males and females were allowed to emerge separately.

Intracellular cAMP levels

Compounds found to inhibit pheromone production in vivo by at least 50% were subsequently analyzed using the assay for cAMP production by intersegmental membranes. Ovipositor tips, consisting of the eighth and ninth abdominal segments with the attached intersegmental membrane, were removed during the 10–12th hr photophase from 2- or 3-day-old females. The intersegmental membranes were isolated by dissection and washed twice in PIPES-buffered physiological medium (21 mM KCl, 12 mM NaCl, 3 mM $CaCl_2$, 18 mM $MgCl_2$, 85 mM glucose, and 43 mM trehalose in 5 mM PIPES buffer brought to pH 6.6 with 0.1 N KOH). The intersegmental membranes were incubated in 10 μl of medium containing isobutylmethylxanthine at 1 μg/μl (Sigma) in the presence of synthetic Hez-PBAN (1 pmol/intersegment/10 μl) and the test compounds for 10 min. The reaction was stopped by transferring the intersegmental membranes into a 1:5 mixture of 20% perchloric acid and HEPES buffer (50 mM) on ice. After incubation on ice for 20 min the intersegmental membranes were homogenized, titrated to pH 7 with 1.5 M KOH, and centrifuged at 2000 $\times$ g for 10 min. The supernatant was removed and used for radioimmunoassay (RIA). The RIA for cAMP was performed as described previously.

COMPUTATIONAL DETAILS

Hypothesis generation

All experiments were conducted on a Silicon Graphics O_2, running under the IRIX 6.3 operating system. Hypothesis generation and its functionality are available as part of the Molecular Simulations Catalyst/Hypo modeling environment. Molecules were edited with the Catalyst 2D/3D visualizer. The Catalyst model treats molecular structures as templates consisting of strategically positioned chemical functions that will bind effectively with complementary functions on receptors. The biologically most important binding functions are deduced from a small set of compounds that cover a broad range of activity. Catalyst automatically generated conformational models for each compound, using the Poling algorithm.[34–36] Diverse conformational models for each compound were generated such that the conformers covered accessible conformational space defined within 20 kcal of the estimated global minimum. The models emphasized conformational diversity under the constraint energy threshold above the estimated global minimum based on use of the CHARMm force field.[34,36,37] Molecular flexibility is taken into account by considering each

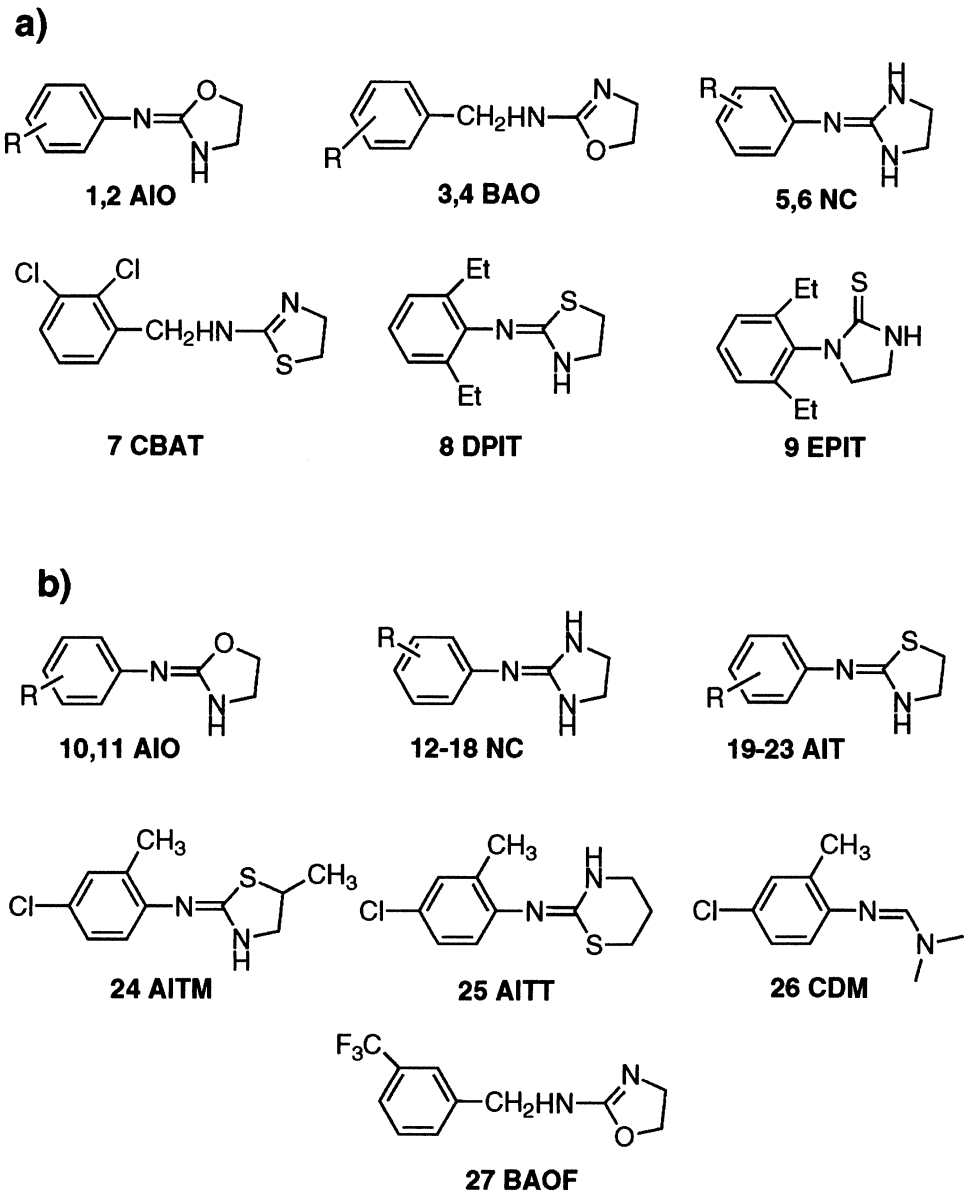

Figure 1. Structures of OA agonists in the (a) training and (b) test sets.

compound as a collection of conformers representing a different area of conformational space accessible to the molecule within a given energy range. Catalyst provides two types of conformational analysis: fast and best quality. The Fast option was used, specifying 250 as the maximum number of conformers.

The molecules associated with their conformational models were submitted to Catalyst hypothesis generation. The present work shows how a set of binding activities of various OA agonists, responsible for the inhibition of sex pheromone production in *H. armigera*, may be treated statistically to uncover the molecular characteristics that are essential for high activity. These characteristics are expressed as chemical features disposed in three-dimensional space and are collectively termed a *hypothesis*. Hypotheses approximating the pharmacophore are described as a set of features distributed within 3D space. This process considered only surface-accessible functions such as hydrogen bond acceptor (HBA), hydrogen bond donor (HBD), hydrophobic (Hp), hydrophobic aliphatic (HpAl), negative charge, positive charge, ring aromatic (RA), negative ionizable (NI), and positive ionizable (PI).[38] A preparative test was performed with these features. NI and PI were used rather than negative charge and positive charge in order to broaden the search for deprotonated and protonated atoms or groups at physiological pH. Furthermore, to emphasize the importance of an aromatic group corresponding to the phenol moiety of test compounds, RA, which consists of directionality, was chosen to be included in the subsequent run. The hypothesis generator was restricted to select only five features, owing to the molecule's flexibility and functional complexity. For molecules larger than dipeptides, Catalyst often will find five-feature hypotheses automatically, but for smaller molecules, three- or four-feature hypotheses might be in the majority. Since hypotheses with more features are more likely to be stereospecific and generally more restrictive models, the total features minimum

value was set to 5 in order to force Catalyst to search for 5-feature hypotheses.[30]

Validation of the hypothesis

During a hypothesis generation run, Catalyst considers and discards many thousands of models. It attempts to minimize a cost function consisting of two terms. One term penalizes the deviation between the estimated activities of the training set molecules and their experimental values; the other term penalizes the complexity of the hypothesis. The overall assumption used is based on Occam's razor, which states that between otherwise equivalent alternatives, the simplest model is best. Simplicity is defined using the minimum description length principle from information theory. The overall cost of a hypothesis is calculated by summing the cost function consisting of three terms (weight cost, error cost, and configuration cost). Weight cost is a value that increases in a Gaussian form as the feature weight in a model deviates from an idealized value of 2.0. Error cost is a major value that increases as the root mean square (RMS) difference between estimated and measured activities. Configuration cost is a fixed cost that depends on the complexity of the hypothesis, and is equal to the entropy of the hypothesis space.

Besides providing a numerical score for each generated hypothesis, Catalyst provides two numbers to help the chemist assess the validity of a hypothesis. One is the cost of an ideal hypothesis, which is a lower bound on the cost of the simplest possible hypothesis that still fits the data perfectly. The other is the cost of the null hypothesis, which presumes that there is no statistically significant structure in the data, and that the experimental activities are normally distributed about their mean. Generally, the greater the difference between the two costs, the higher the probability for finding useful models. In terms of hypothesis significance, a generated hypothesis with a cost that is substantially below that of the null hypothesis is likely to be statistically significant and bears visual inspection.[39]

ASSESSMENT OF 3D QSAR FOR INHIBITORY ACTIVITY

A set of nine molecules that are responsible for the inhibition of sex pheromone production in *H. armigera* was selected as the target training set. Their chemical structures and experimental activities are listed in Figure 1a and Table 1. NC derivative substituted with 2,6-$(CH_3)_2$ (**6**) had the highest potency, followed by AIO 2-CH_3,4-Cl_2 (**1**) and NC 2,6-Cl_2 (**5**) in inhibition of cAMP production by 1 pmol of PBAN/intersegment/10 μl (Table 1). Affinities of the agonists are expressed as their K_i values in nanomolar units and activities range over four orders of magnitude (minimum, 3.85 nM; and maximum, 100 000 nM). This set included a variety of types of molecules and for this type of training set, the use of the hypothesis generation tool was appropriate. This tool builds hypotheses (overlays of chemical features) for which the fit of individual molecules to a hypothesis can be correlated with the molecule's affinity.

The 3D-QSAR study was performed with the Catalyst (version 3.1) package. The geometry of each compound was built with a visualizer and optimized by using the generalized CHARMm-like force field[21–24] implemented in the program. It was found that hypotheses contain good correlation with HBA, Hp, and HpAl. The characteristics (cost, RMS, and the regression constant r) of the 10 lowest cost hypotheses are listed in Table 2. The statistical relevance of the various hypotheses obtained is assessed on the basis of their cost relative to the null hypothesis and their correlation coefficients r.[30] The total fixed cost of the run is 34.98 and the cost of the null hypothesis is 85.10. The cost range between best hypothesis 1 and null hypothesis is 36.97. The cost range over the 10 generated hypotheses is 15.66. Hypotheses 1, 3, 6, 7, and 9 consist of the same chemical feature functions as an HBA, three Hps, and an HpAl feature. The second group is composed of hypotheses 2 and 8, which are characterized by an HBA and four Hps. Other hypotheses (4, 5, and 10) are characterized by an HBA, two Hps, and two HpAl features. Comparison of procedure and regression studies showed that hypotheses 1, 2, and 4 are the

Table 1. Predicted activity from 10 best hypotheses against actual inhibitory activity data for 9 agonists

Compound				Hypotheses									
No.	R	Exp.	Conf.	1	2	3	4	5	6	7	8	9	10
1	AIO 2-CH_3, 4-Cl	6.15	15	4.5	3.7	4.4	4.8	3.4	2.7	3.2	4	200	180
2	AIO 2-CH_3, 6-CH_2CH_3	6 150	12	210	260	270	190	270	340	170	110	41	34
3	BAO 2-F	100 000	51	120 000	110 000	170 000	180 000	150 000	37 000	130 000	190 000	53 000	76 000
4	BAO 3,5-Cl_2	69.2	51	160	110	140	220	750	1 000	910	120	330	3 000
5	NC 2,6-Cl_2	8.97	29	38	48	45	36	40	42	53	68	7.5	9.9
6	NC 2,6-$(CH_3)_2$	3.85	31	38	52	47	36	36	37	57	72	5.2	6.2
7	CBAT	76 900	187	5 600	6 200	4 500	4 400	1 900	2 800	2 900	3 800	3 900	3 400
8	DPIT	61.5	42	110	100	100	100	140	160	94	330	380	260
9	EPIT	5 380	35	14 000	12 000	85 000	11 000	5 700	9 500	4 500	3 600	2 900	3 100

Abbreviations: Exp., experimental data (K_i in nM in inhibition of cAMP production by 1 pmol of PBAN/intersegment/10 μl); Confs., number of conformational models.

best models among the three groups and were selected for further evaluation.

VALIDATION OF THE HYPOTHESIS

The hypotheses are used to estimate the activities of the training set. Those activities are derived from those conformers displaying the smallest RMS deviations when projected onto the hypothesis. Hypotheses 1, 2, and 4 shared five common features located at almost exactly the same 3D coordinates. The quality of the correlation among the data in the training set is given by the RMS score, which was normalized by the log (uncertainty) and by *r*. All calculated activities from the 10 best hypotheses and the number of generated conformations for each molecule are listed in Table 1. Even though hypothesis 1 has a lower cost value than hypotheses 2 and 4 (34.98, 48.17, and 48.44 for hypotheses 1, 2, and 4, respectively), they have nearly no difference in *r* and RMS. The RMS index for hypothesis 1 is very small (1.594) and those for hypotheses 2 and 4 are 1.584 and 1.658, respectively. Roughly speaking, the greater the difference between the cost of the generated hypothesis and that of the null hypothesis, the more likely it is that the hypothesis reflects a chance correlation.[39] The correlation between observed and estimated binding activities is satisfactory in the three hypotheses. The predicted activities are in the right order and parallel the values actually observed (Table 1).

The small cost range observed here may be due to two factors, that is, the molecules in the training set are fairly rigid and have a high degree of structural homology. Owing to the relatively small range between the costs for an ideal versus null hypothesis and owing, moreover, to the placement of the identified hypotheses within this range, special care was taken to test for chance correlation. Hypothesis 1 turns out to be the best measure in the test set for the whole training set as attested by the reasonably good correlation between observed and estimated activities (cost = 48.13, cost of the null hypothesis = 85.10). Hence, hypothesis 1 was regressed using each molecule in its most chemically reasonable conformation (Figure 2). AIO (**2**) and CBAT (**7**) were underestimated by hypothesis 1, which had the highest statistical correlation ($r = 0.894$) and the smallest error value (RMS = 1.594). The number of compounds used in preparing the Catalyst hypotheses is so small (only 9) that it will need improvement to design new molecules.

RECEPTOR–DRUG INTERACTION

QSAR modeling is an area of research pioneered by Hansch and Fujita.[40,41] QSAR attempts to model the activity of a series of compounds by using measured or computed properties of the compounds. More recently, QSAR has been extended by including three-dimensional information. In drug discovery, it is common to have measured activity data for a set of compounds acting on a particular protein but not to have knowledge of the three-dimensional structure of the active site. In the absence of such three-dimensional information, one can attempt to build a hypothetical model of the receptor site that can provide insight about receptor site characteristics. Such a model is known as a Hypo, which provides three-dimensional information about a putative receptor site. Catalyst/Hypo was useful in building 3D pharmacophore models from the binding activity data and conformational structure. It can be used as an alternative for QSAR methods.

Color Plate 1a–c depicts one of the most active conformations of **1** in the training set mapped onto the lowest cost hypothesis 1, on the second lowest cost hypothesis 2, and on the fourth lowest cost hypothesis 4, respectively. The molecule maps well onto all five hypothesis features in a similar way (see Color Plate 1a–c) and therefore these hypotheses are considered to be equivalent. In hypothesis 1, one Hp of hypothesis 2 is replaced by an HpAl and in hypothesis 4 another Hp of hypothesis 1 is replaced by an HpAl. Roughly speaking, hypotheses 1, 2, and 4 have good similarity in 3D spatial shape. The phenyl group of **1** overlaps with the Hp feature of hypothesis 1, whereas the bridge nitrogen atom serves as an HBA between a phenyl and imidazolidine ring. The pair of Hp features overlap neatly with the 2-methyl group and 4-chlorine atom, respectively, and an HpAl is disposed over the oxazolidine ring. Thus, one of the most active OA agonists in the training set, **1**, maps closely with the statistically most significant hypothesis 1, which is characterized by five features (Color Plate 1a) and the predicted activity of **1** by hypothesis 1 is reasonable (Table 1). Catalyst may be somewhat insensitive to halogenation on aromatic rings, since an Hp feature overlaps usually with a methyl group, such as in **2** and **6**, whereas in **1**, the pair of Hp features overlap with the 2-methyl group and 4-chlorine atom, respectively.

One Hp feature of hypothesis 1 does not fit with AIO **2**, an

Table 2. Characteristics of 10 lowest cost hypotheses from 9 OA agonists (cost of ideal hypothesis: 34.98, cost of null hypothesis: 85.10)

Hypothesis	Feature 1	Feature 2	Feature 3	Feature 4	Feature 5	Cost	RMS	*r*
1	HBA	Hp 1	Hp 2	Hp 3	HpAl 1	48.13	1.594	0.894
2	HBA	Hp 1	Hp 2	Hp 3	Hp 4	48.17	1.584	0.896
3	HBA	Hp 1	Hp 2	Hp 3	HpAl 1	48.43	1.605	0.893
4	HBA	Hp 1	Hp 2	HpAl 1	HpAl 2	48.44	1.658	0.882
5	HBA	Hp 1	Hp 2	HaAl 1	HpAl 2	51.63	1.861	0.849
6	HBA	Hp 1	Hp 2	Hp 3	HpAl 1	52.79	1.846	0.858
7	HBA	Hp 1	Hp 2	Hp 3	HpAl 1	53.11	1.956	0.831
8	HBA	Hp 1	Hp 2	Hp 3	Hp 4	53.15	1.961	0.830
9	HBA	Hp 1	Hp 2	Hp 3	HpAl 1	63.79	2.453	0.713
10	HBA	Hp 1	Hp 2	HpAl 1	HpAl 2	63.79	2.445	0.716

Abbreviations: HBA, hydrogen bond acceptor; Hp, hydrophobic; HpAl, hydrophobic aliphatic.

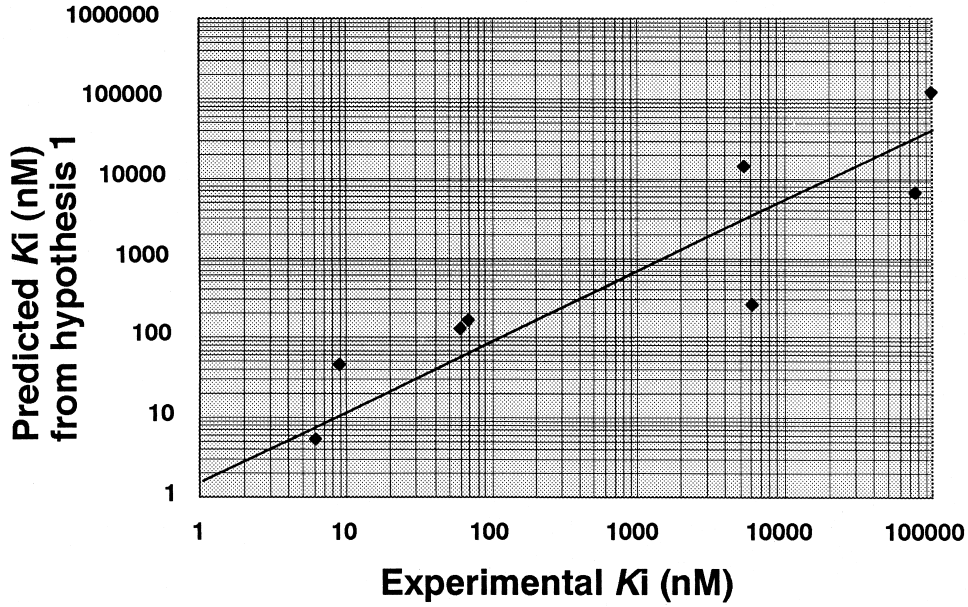

Figure 2. Plot of predicted activities against experimental values (K_i in nanomolar units).

analog of **1** (Color Plate 2a), and thus **2** is less active than **1** (Table 1). BAO **3**, with the lowest activity in the training set (experimental, 100 μM), fits only two features of hypothesis 1 (Color Plate 2b). A distinguishing characteristic of hypothesis 1 is that it underestimated the activity of **6** (experimental, 3.85 nM; estimated, 38 nM), the most active OA agonists in the training set, and similarly all other hypotheses predicted a little lower activity for **6** than that for the experimental value. This result may also imply that Catalyst does not treat **6**-like structures reasonably in the process of calculating a hypothesis. The mapping of **6** onto hypothesis 1 (Color Plate 2c) showed that one Hp feature of hypothesis 1 does not fit with **6**. Thus, the present studies on OA agonists demonstrate that an HBA site and four hydrophobic sites located on the molecule seem to be essential to inhibit cAMP production by 1 pmol of PBAN/intersegment/10 μl of *H. armigera*. The result resembles that of binding activity to locust OAR3,[32] in which an HBA site and four hydrophobic sites located on the molecule also seem to be essential in binding of OA agonists to OAR3. The phenyl moiety, 4-substituent, and imidazolidine ring of the most active compound as OA agonist to OAR3 overlaps with the three Hp features of hypothesis 1, whereas the bridge nitrogen atom, between phenyl and imidazolidine rings, serves as an HBA. The HpAl feature overlaps neatly with the 2-substituent. Generally, more active molecules map onto all of the features of the hypothesis. Conversely, compounds that are estimated to have low activity map poorly to the hypothesis.

The predictive character of this five-feature hypothesis was further assessed with candidate molecules, whose OA agonist activities are to be examined and whose structures are shown in Figure 1b, outside of the training set. The experimental value is available for compound **27** only in the test set. The best statistically significant hypothesis 1 was applied to access some OA agonists. The predicted values of the most active molecules are listed in Table 3. AIO, NC, and AIT compounds were potent, while BAO compounds were less active. The predicted activity of **27**, according to hypothesis 1, was 1.5 μM and the experimental value was more than 100 μM. One of the reasons why this prediction is so bad may be that the number of compounds used in preparing the Catalyst hypothesis is so small (only nine); this will need improvement to design new molecules. For example, compounds **3** and **4** belong to the same BAO type, but the activity is diverse (100 and 0.0692 μmol); however, they are the only available BAO compounds with known activity so far. It is necessary to include various types of compounds with a variety of activity to obtain better hypotheses and predictions before designing new molecules. Thus, hypothesis 1 is being considered for use in designing new leads for more active compounds. BAOs, whose bridges are longer compared with those of AIO, NC, and AIT (by means of a methylene group between the phenyl and oxazoline rings), do not fit the hypothesis model (Color Plate 2b). Meanwhile, AIOs, whose bridges are shorter than those of BAOs, are suitable for the hypothesis (Color Plate 1a). Assuming that AIOs and AIT have the same tendency, a nitrogen bridge between a phenyl and heterocycle of AIO, NC, and AIT could play an important role. EPIT (**9**) has phenyl and imidazolidine rings directly connected and, thus, is less flexible than its AIT isomer DPIT (**8**), because **9** has less (35) conformational flexibility than that (42) of **8**. Considering that **8** is much more active than **9**, a nitrogen bridge of **8** could be important. Thus, further research on the comparison of the 3D hypotheses from more potent OA agonists as well as those generated from the corresponding data from various insect might be interesting and stimulate further investigation of the mechanisms of OA receptor–ligand interactions.

CONCLUSIONS

Clonidine has been reported to be the strongest inhibitor in inhibition of cAMP production by 1 pmol of PBAN/intersegment/10 μl of *H. armigera*.[11–13] In this report, more active OA agonists, **1** and **6**, were introduced. Three-dimensional pharmacophore hypotheses were built from a training set of nine OA agonists including clonidine (**1**) and

Table 3. Predicted activity of OA agonists from hypothesis 1

Compound		Confs.	Predicted activity (nM in inhibition of cAMP production by 1 pmol of PBAN/intersegment/10 μl)
No.	R		
10	AIO 2-CH_3, 4-I	6	4.5
11	AIO 2,3,4-Cl_3	9	10
12	NC 2,4-Cl_2	18	6.5
13	NC 2-CH_3, 4-Cl	17	1.3
14	NC 2,4-$(CH_3)_2$	15	0.76
15	NC 2,4,5-Cl_3	25	0.42
16	NC 2,4,6-Cl_3	19	4.6
17	NC 2,4,6-$(CH_3)_3$	23	7
18	NC 2,4,6-$(CH_2CH_3)_3$	106	4.4
19	AIT 2,4-Cl_2	9	8.6
20	AIT 2-CH_3, 4-Br	8	7.4
21	AIT 2-CH_3, 4-Cl	11	7.3
22	AIT 2-CH_3, 4-I	8	5
23	AIT 2,4,5-Cl_3	13	4
24	AITM	11	2.6
25	AITT	8	1.4
26	CDM	7	8.9
27	BAOF	76	1 500

Confs., Number of conformational models. The experimental value of **27** was more than 100 μM.

compound **6**. Hypotheses were obtained from this study and applied to map with the active or inactive compounds to explain the mechanism of OA receptor–ligand interactions. Important features were found such as HBA, Hp, and HpAl of the surface-accessible models. An HBA and four hydrophobic features are the minimum components of an effective OA agonistic binding hypothesis, which resembles the results of binding activity to locust OAR3. It was found that more active agonists map well onto all the features of the hypotheses; meanwhile for some inactive compounds, their lack of binding affinity is primarily due to their inability to achieve an energetically favorable conformation shared by the active compounds in order to fit the 3D common feature pharmacophore keys.

On the basis of this study, several three-dimensional pharmacophore models for the OA agonist–receptor interactions have been proposed. These hypotheses are considered to be useful in designing new leads for more active compounds, although the number of compounds tested is still limited. Hence, a further comparison study of 3D hypothesis models of agonists responsible for the inhibition of sex-pheromone production in *H. armigera* is in progress and expected to clarify the mode of action of these compounds acting on the OA receptor. Such work will surely help elucidate the mechanisms of OA receptor–ligand interactions. The preceding hypothesis studies show that agonists with certain substituents can be potential ligands to OA receptors. They may help to point the way in developing extremely potent and relatively specific OA agonists, leading to potential pest control agents. To optimize the activities of these compounds as OA agonists, more detailed experiments are in progress.

ACKNOWLEDGMENTS

This work was supported in part by a Grant-in-Aid for Scientific Research from the Ministry of Education, Science, and Culture of Japan.

REFERENCES

1 Raina, A.K. Neuroendocrine control of sex pheromone biosynthesis in Lepidoptera. *Annu. Rev. Entomol.* 1993, **38**, 329–349

2 Ma, P.W.K., and Roelofs, W. Calcium involvement in the stimulation of sex pheromone production by PBAN in the European corn borer, *Ostrinia nubilalis* (Lepidoptera: Pyralidae). *Insect Biochem. Mol. Biol.* 1995, **25**, 467–473

3 Rafaeli, A., and Gileadi, C. Neuroendocrine control of pheromone production in moths. *Invertebr. Neurosci.* 1997, **3**, 223–229

4 Jurenka, R.A. Signal transduction in the stimulation of sex pheromone biosynthesis in moths *Arch. Insect Biochem. Physiol.* 1996, **33**, 245–258

5 Soroker, V., and Rafaeli, A. *In vitro* hormonal stimulation of acetate incorporation by *Heliothis armigera* pheromone glands. *Insect Biochem.* 1989, **19**, 1–9

6 Rafaeli, A., Soroker, V., Kamensky, B., and Raina, A.K. Action of PBAN on *in vitro* pheromone glands of *Heliothis armigera* females. *J. Insect Physiol.* 1990, **36**, 641–646

7 Arima, R., Takahara, K., Kadoshima, T., Numazaki, F., Ando, T., Uchiyama, M., Nagasawa, H., Kitamura, A., and Suzuki, A. Hormonal regulation of pheromone biosynthesis in the silkworm moth *Bombyx mori* (Lepidoptera: Bombycidae). *Appl. Entomol. Zool.* 1991, **26**, 137–148

8 Jurenka, R.A., Jacquin, E., and Roelofs, W.L. Stimulation of pheromone biosynthesis in the moth *Helicoverpa zea*: Action of a brain hormone on pheromone glands involves Ca^{2+} and cAMP as second messengers. *Proc. Natl. Acad. Sci. U.S.A.* 1991, **88**, 8621–8625
9 Fonagy, A., Matsumoto, S., Schoofs, L., De Loof, A., and Mitsui, T. *In vivo* and *in vitro* pheromonotropic activity of two locustatachykinin peptides in *Bombyx mori*. *Biosci. Biotech. Biochem.* 1992, **56**, 1692–1693
10 Matsumoto, S., Ozawa, R., Nagamine, T., Kim, G.-H., Uchiumi, K., Shono, T., and Mitsui, T. Intracellular transduction in the regulation of pheromone biosynthesis of the silkworm, *Bombyx mori:* Suggested involvement of calmodulin and phosphoprotein phosphatase. *Biosci. Biotech. Biochem.* 1995, **59**, 560–562
11 Rafaeli, A., and Gileadi, C. Modulation of the PBAN-induced pheromonotropic activity in *Helicoverpa armigera*. *Insect Biochem. Mol. Biol.* 1995, **25**, 827–834
12 Rafaeli, A., and Gileadi, C. Down regulation of pheromone biosynthesis: Cellular mechanisms of pheromonostatic responses. *Insect Biochem. Mol. Biol.* 1996, **26**, 797–807
13 Rafaeli, A., Gileadi, C., Fan, Y., and Meixun, C. Physiological mechanisms of pheromonostatic responses: Effects of adrenergic agonists and antagonists on moth pheromone biosynthesis. *J. Insect Physiol.* 1997, **43**, 261–269
14 Axelrod, J., and Saavedra, J.M. Octopamine. *Nature (London)* 1977, **265**, 501–504
15 Evans, P.D. In: *Reviews in Comparative Molecular Neurobiology* (S.R. Heller, ed.). Birkhäuser Verlag, Basel, 1993, pp. 287–296
16 Evans, P.D. In: *Reviews in Comprehensive Insect Physiology Biochemistry Pharmacology* (G.A. Kerkut and G. Gilbert, eds.), Vol. 11. Pergamon Press, Oxford, 1985, pp. 499–530
17 Nathanson, J.A. Phenyliminoimidazolidines. Characterization of a class of potent agonists of octopamine-sensitive adenylate cyclase and their use in understanding the pharmacology of octopamine receptors. *Mol. Pharmacol.* 1985, **28**, 254–268
18 Evans, P.D. Multiple receptor types for octopamine in the locust. *J. Physiol.* 1981, **318**, 99–122
19 Roeder, T., and Nathanson, J.A. Characterization of insect neuronal octopamine receptors (OA3 receptors). *Neurochem. Res.* 1993, **18**, 921–925
20 Roeder, T., and Gewecke, M. Octopamine receptors in locust nervous tissue. *Biochem. Pharm.* 1990, **39**, 1793–1797
21 Roeder, T. A new octopamine receptor class in locust nervous tissue, the octopamine 3 (OA3) receptor. *Life Sci.* 1992, **50**, 21–28
22 Roeder, T. Pharmacology of the octopamine receptor from locust central nervous tissue (OAR3). *Br. J. Pharmacol.* 1995, **114**, 210–216
23 Roeder, T. High-affinity antagonists of the locust neuronal octopamine receptor. *Eur. J. Pharmacol.* 1990, **191**, 221–224
24 Jennings, K.R., Kuhn, D.G., Kukel, C.F., Trotto, S.H., and Whiteney, W.K. A biorationally synthesized octopaminergic insecticide: 2-(4-Chloro-*o*-toluidino)-2-oxazoline. *Pestic. Biochem. Physiol.* 1988, **30**, 190–197
25 Hirashima, A., Yoshii, Y., and Eto, M. Action of 2-aryliminothiazolidines on octopamine-sensitive adenylate cyclase in the American cockroach nerve cord and on the two-spotted spider mite *Tetranycus urticae* Koch. *Pestic. Biochem. Physiol.*, 1992, **44**, 101–107
26 Ismail, S.M.M., Baines, R.A., Downer, R.G.H., and Dekeyser, M.A. Dihydrooxadiazines: Octopaminergic system as a potential site of insecticidal action. *Pestic. Sci.* 1996, **46**, 163–170
27 Hirashima, A., Shinkai, K., Pan, C., Kuwano, E., Taniguchi, E., and Eto, M. Quantitative structure–activity studies of octopaminergic ligands against *Locust migratoria* and *Periplaneta americana. Pestic. Sci.* 1999, **55**, 119–128
28 Pan, C., Hirashima, A., Tomita, J., Kuwano, E., Taniguchi, E., and Eto, M. Quantitative structure–activity relationship studies and molecular modelling of octopaminergic 2-(substituted benzylamino)-2-thiazolines and oxazolines against nervous system of *Periplaneta americana* L. *Internet J. Sci.-Biol. Chem.* 1997, **1**, http://www.netsci-journal.com/97v1/97013/index.htm.
29 Hirashima, A., Pan, C., Tomita, J., Kuwano, E., Taniguchi, E., and Eto, M. Quantitative structure–activity studies of octopaminergic agonists and antagonists against nervous system of *Locusta migratoria. Bioorg. Med. Chem.* 1998, **6**, 903–910
30 Molecular Simulations. *Catalyst Tutorial*, version 4.0. Molecular Simulations, Inc., San Diego, California, 1998
31 Pan, C., Hirashima, A., Kuwano, E., and Eto, M. Three-dimensional pharmacophore hypotheses for the locust neuronal octopamine receptor (OAR3). 1. Antagonists. *J. Mol. Modelling* 1997, **3**, 455–463
32 Hirashima, A., Pan, C., Kuwano, E., Taniguchi, E., and Eto, M. Three-dimensional pharmacophore hypotheses for the locust neuronal octopamine receptor (OAR3). 2. Agonists. *Bioorg. Med. Chem.* 1999, **7**, 1437–1443
33 Rafaeli, A., Gileadi, C., and Hirashima, A. Identification of novel octopamine agonists responsible for the inhibition of moth sex pheromone production. *Pestic. Biochem. Physiol.* 1999, in press
34 Smellie, A., Teig, S.L., and Towbin, P. Poling-promoting conformational variation. *J. Comput. Chem.* 1995, **16**, 171–187
35 Smellie, A., Kahn, S.D., and Teig, S.L. Analysis of conformational coverage. 1. Validation and estimation of coverage. *J. Chem. Inf. Comput. Sci.* 1995, **35**, 285–294
36 Smellie, A., Kahn, S.D., and Teig, S.L. Analysis of conformational coverage. 2. Application of conformational models. *J. Chem. Inf. Comput. Sci.* 1995, **35**, 295–304
37 Brooks, B.R., Brucolleri, R.E., Olafson, B.D., States, D.J., Swaminathan, S., and Karplus, M. CHARMm: A program for macromolecular energy, minimization, and dynamics calculations. *J. Comput. Chem.* 1983, **4**, 187–217
38 Greene, J., Kahn, S., Savoj, H., Sprague, P., and Teig, S. Chemical function queries for 3D database search. *J. Chem. Inf. Comput. Sci.* 1994, **34**, 1297–1308
39 Hoffmann, R., and Bourguignon., J.-J. Building a hypothesis for CCK-B antagonists. 1. Peptoids. In: *Complete Listing of Case Studies by Application Area*. Molecular Simulations Inc. http://www.msi.com/solutions/cases/notes/CCKB−Pep−full.html
40 Hansch, C., and Leo, A. In: *Exploring QSAR: Fundamentals and Applications in Chemistry and Biochemisry*. American Chemical Society, Washington, D.C., 1995
41 Hansch, C., and Fujita, T. ρ-σ-π analysis. A method for the correlation of biological activity and chemical structure. *J. Am. Chem. Soc.* 1964, **86**, 1616–1626

Akinori Hirashima, Ada Rafaeli, Carina Gileadi, and Eiichi Kuwano

Three-dimensional pharmacophore hypotheses of octopamine receptor responsible for the inhibition of sex-pheromone production in *Helicoverpa armigera*

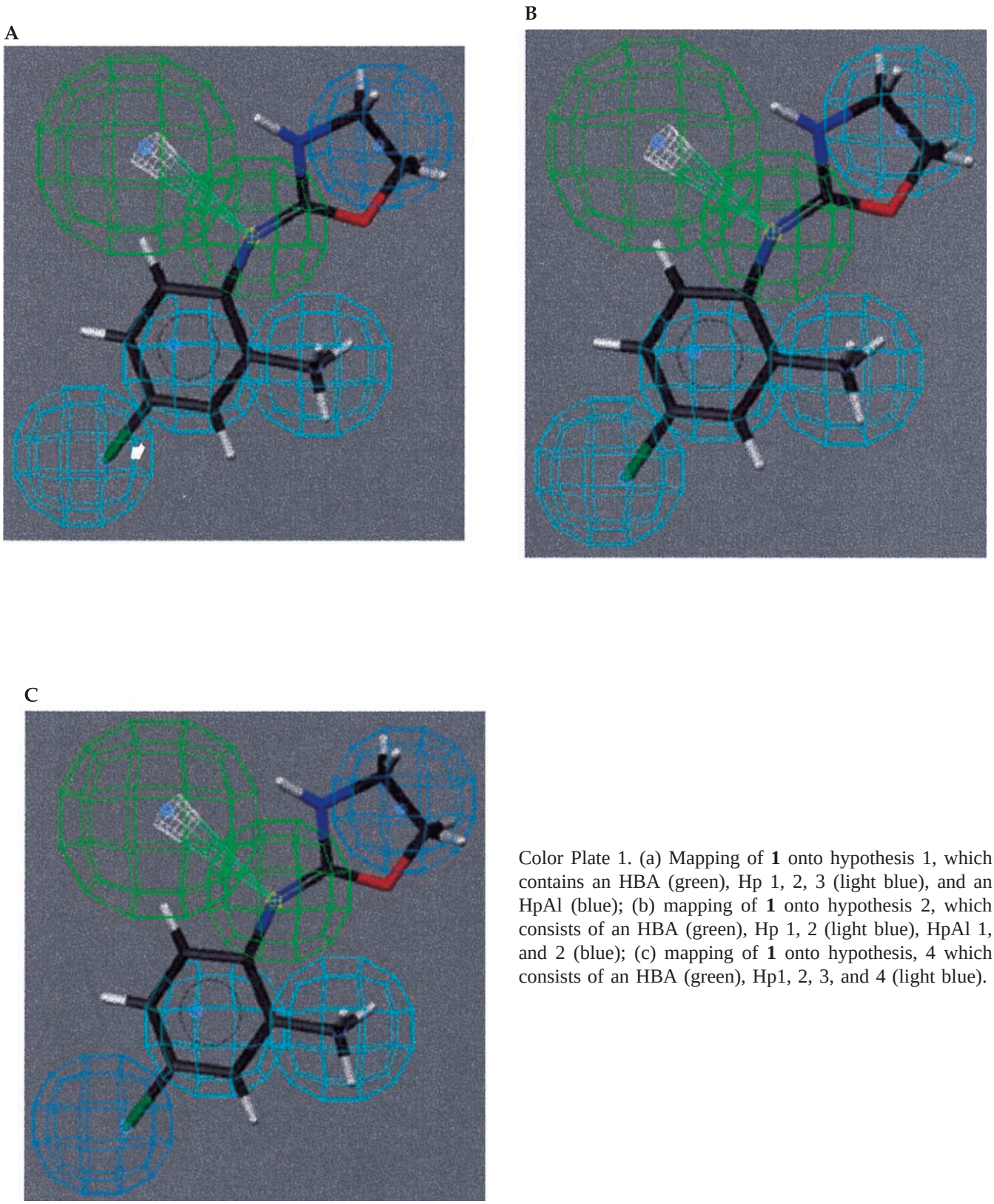

Color Plate 1. (a) Mapping of **1** onto hypothesis 1, which contains an HBA (green), Hp 1, 2, 3 (light blue), and an HpAl (blue); (b) mapping of **1** onto hypothesis 2, which consists of an HBA (green), Hp 1, 2 (light blue), HpAl 1, and 2 (blue); (c) mapping of **1** onto hypothesis, 4 which consists of an HBA (green), Hp1, 2, 3, and 4 (light blue).

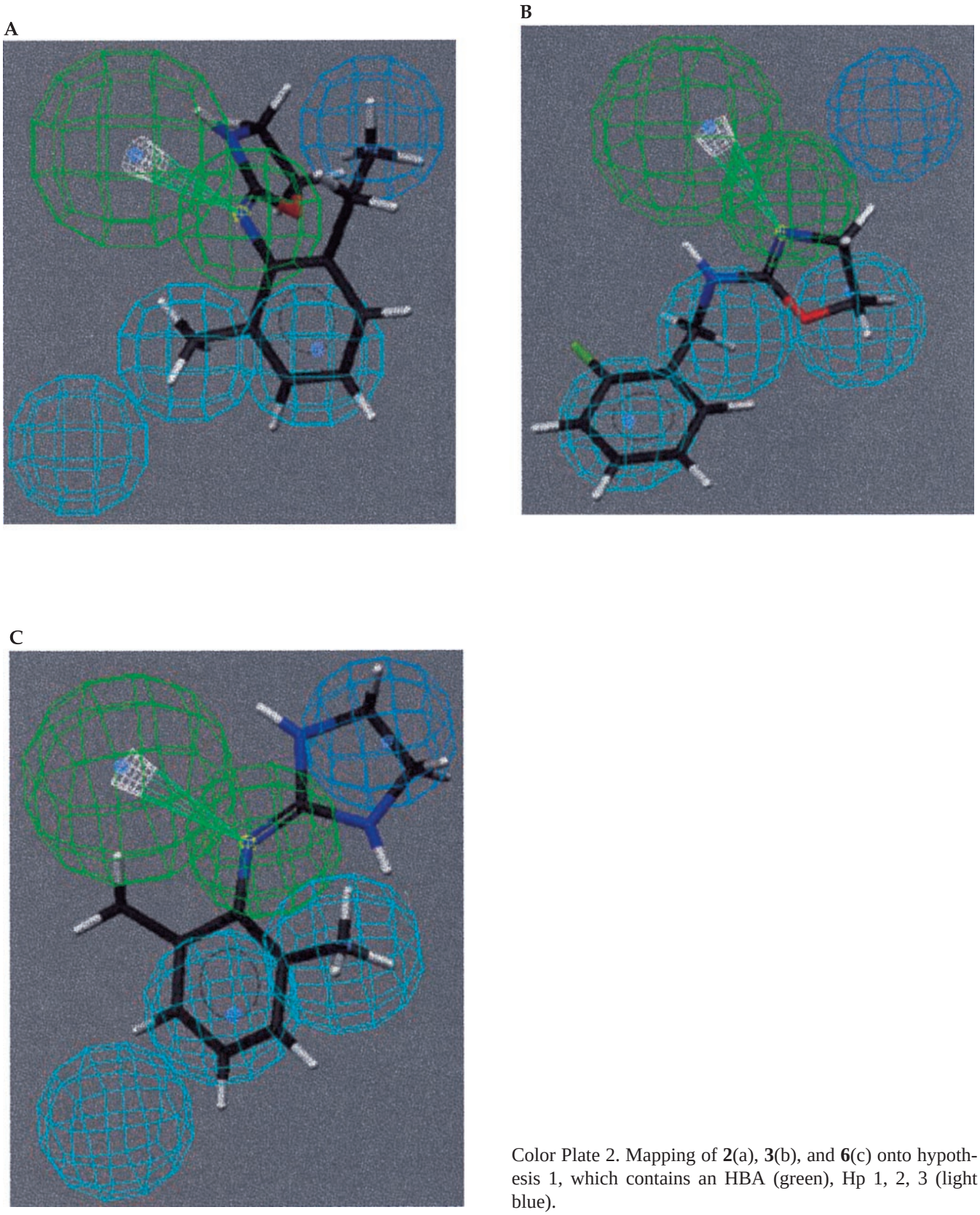

Color Plate 2. Mapping of **2**(a), **3**(b), and **6**(c) onto hypothesis 1, which contains an HBA (green), Hp 1, 2, 3 (light blue).